International Journal of Research in Engineering and Science (IJRES)
ISSN (Online): 2320-9364, ISSN (Print): 2320-9356
www.ijres.org Volume 7 Issue 3 Ser. I ǁ 2019 ǁ PP. 01-16

Small strain stiffness of loessic soils across South East England

Haaris Nobee-Fox[*1], Arya Assadi-Langroudi[2]
[*1]*Graduate, Civil Engineering, University of East London, England, United Kingdom*
[*1] *Senior Lecturer in Geomechanics, Civil Engineering, University of East London, England, United Kingdom*
Corresponding Author: Haaris Nobee-Fox

ABSTRACT: *Loess soils, commonly known as brickearth in the UK, have been modestly distributed across South, East, and South East England and are typically reworked with limited collapsibility. The High Speed Rail 2 alignment will cut in to Buckinghamshire and Hertfordshire where loess and loess-like drifts have been distributed in pockets. Serviceability of the high speed transportation infrastructure is dependent on soil small strain stiffness, G_{max} . Little is known about the magnitude and variation of G_{max} with depth, and its relevance to mineralogical variations of loess across the regions and along depth profiles.In this paper, a series of vertical profiles for G_{max} in lower and upper loessic sequences of South East England are generated using systematically collated semi-empirical equations and ground investigation data. Profiles are then contrasted with in-situ measured shear wave velocityand G_{max} . Discrepancy between measured and derivedG_{max} are discussed and general implications are drawn out. Findings from this research inform ground and geotechnical engineers with an interest in performance-based design of engineered earth systems on loess and advanced HS and HSS soil models.*

Date of Submission: 21-08-2019 Date of acceptance:05-09-2019

I. INTRODUCTION

Loess soil is deemed stable as long as it is not disturbed through loading, wetting, or a combination of the two. This is due to the cemented, openly-packed structure of loess, placing it in a transitional state which allows conditional stability. If the conditions change then this stability can be lost and the soil may collapse (Barden, McGown and Collins, 2018).At micro-scale, interlocking between particlesand cementation tend to holdtogether the quartz silt and sand particles in loess;changesininterparticle forces and the total environment may lead to contact modification, instability, and sudden collapse.

Pore spaces and their distribution play a key role in stability of loess. The micro-structure of loess includes three types of pores:trans-assemblage pores also known as trellis pores, and intra-assemblage pores which can range from micro to macro pores surrounded by chains of fine sand and silt particles. When multiple silt particles sit together via direct grain-grain contact or soluble connectors (e.g. salts and clays), trellis pores(Fig. 1) form which typically size larger than meansilt diameter and are broadly known as metastable voids prone to collapse and sudden settlement. Prolonged consolidation, wetting, loading and seismic excitation can compress these pores, remove or relax the collapsibility. The proportion of trellis pores that fail during service life of engineered loess is dependent on type of cementing agents that loess contains, the grading quality of loess frame elements (i.e. sand and silt), and the pore anatomy (i.e. pore size distribution).

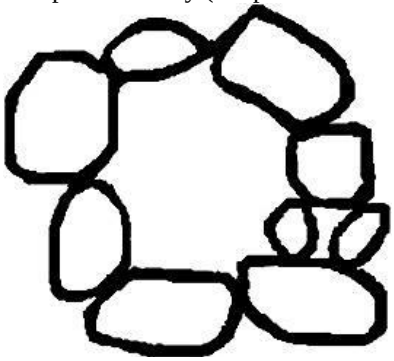

Fig.1 trellis pores or trans-assemblage voids surrounded by chain of frame elements in loess (Lin, 1960)

A grand global challenge in the world of geomechanics has been to tackle the problem of loess collapsibility and risk associated with buildingon or intoloessdue to its potential to collapse, swell, and cyclic volume change; these can be serious geotechnical hazards. Recent seminal studies such as Yuan and

Wang(2009)have found a relationship between the collapsibility of loess and settlement induced by seismic excitation; whilst the triggering mechanism may vary, the metastable microstructure of loess controls the behaviour in both cases. The primary trigger for collapsibility is loss of suction, and seismic settlement is the result of shear failure of the loess matrix under dynamic loads; both of these will result in the collapse of trellis pores.

1.1 MICROMECHANICS OF COLLAPSE IN LOESS

Micro-pores between trellis pores generate the suction needed to give the loess its apparent strength. The loss of these pores will result in structural collapse. The higher the sand content in loess, the less likely the collapsibility due to reduced probability of formations of trellis pore. Figure 2a plots the collapsibility potential (i.e. collapse settlement divided by depth of collapsible loess profile)against sand contact in loess. For clay fraction however, an increase in the clay content in loess (that already has low clay content) can increase the chance of collapse. An increase in clay content lowers the likelihood of collapsibility in very clayey loess. This is due to the clay fraction occupying the trellis pores, a general decrease in volume of macro-pores at the expense of growth in number of micro-pores and suction. Figure 2b shows how sand and clay impacts the collapsibility of loess.

The presence of salt (carbonates, sulphates, oxides, and alike) in loess can affect the collapsibility: When loess becomes saturated the salt component may dissolve, leading to contact modification and collapse. For calcareous clayey loess, Assadi-Langroudi and Jefferson (2013) showed a wetted induced decrease in maximum pore size from 76 µm to 42 µm, aggregation of sub 20 µm particles, and a reduction in volume of micro-pores (0.3-1.5 µm and 0.001-0.25 µm) upon expansion of the clay fraction. The latter has direct implication on soil water retention and hysteresis response of loessic soils (also see Munoz-Castelblanco et al., 2012). Collapse may be triggered on loss of suction. Suction plays a key role in soils strength; the loss of suction impacts trellis pores and produces an effect similar to micro-shear, causing large deformations.Generally, the finer the soil grains, the higher the liquid limit, and the higher the suction value, suggesting great reliance of stability of loess on suction. Suction is also controlled by the average pore space size in soil; the smaller the pore sizes, the higher the suction. As loess is made up of mostly fine grained granular maters (i.e. fine sand and silt, with a pronounced size of 10 to 20µm), smaller pores generally render higher levels of suction. Even though the trellis pores and the macro-pores are typically larger than the mean diameter of loess frame elements (i.e. silt and fine sand), chains of sand and silt particles around these pores connected by cementing agents (clay/calcium carbonate/oxide), and the constituting micro-pores forming these cementing agents develop high levels of suction. As such, the greater the number of trellis and macro-pores can lead to greater population of micro-pores, and hence suction. This highlights the importance of the trellis pores in regards to maintaining the loess structure.

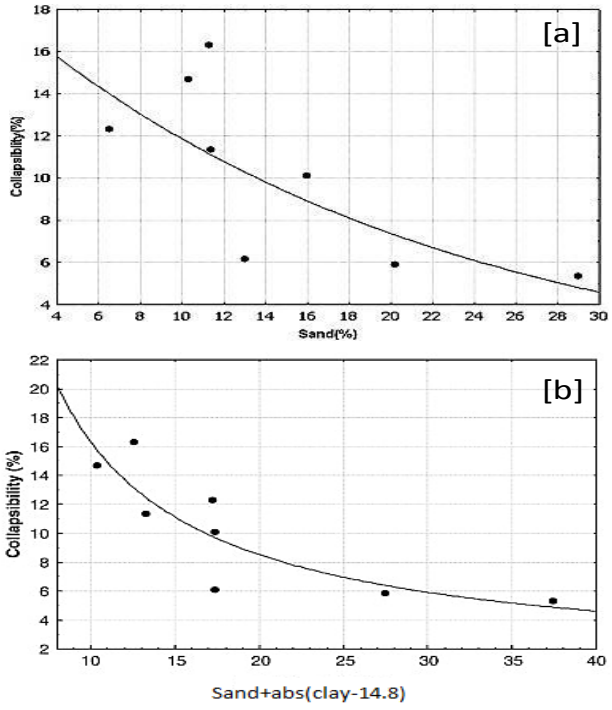

Fig. 2[a] variation of collapsibility with sand content (Yuan and Wang, 2009), [b] variation of collapsibility with sand and clay content (Yuan and Wang, 2009)

Dynamicexcitation

Collapsein loess upon dynamic excitation is affected by loess water content, dry density, and dynamic load characteristics including frequency, magnitude, and duration. Dynamic loading and seismic settlement share a proportional relationship with each other, meaning the stronger and longer load is applied to loess, the larger the resulting seismic settlement will be.

Studies conducted by Wang et al., (2000)show that there is a relationship between dry density of loess that has undergone compaction and level of settlement produced as a result of dynamic loading. It was found that the higher the dry density of the compact loess, the less settlement the loess develops under dynamic compaction; though this relationship does reach a threshold where loess cannot be improved any further to resist seismic settlement.

The degree of saturation in the soil when measuring seismic settlement plays a key factor here as shown in Wang et al., (2012) where undisturbed loess was tested to identify the relationship between damping ratio and dynamic shear modulus. It was found that the higher the water content in the soil the more settlement the loess would undergo. This is probably because higher water content lowersinter-particle friction, resulting in higher seismic settlement. This internal friction consumes energy during the deformation of loess, which can be used as a representation of the energy loss during earthquakes indicating the reduction of the seismic waves. High speed vehicles generate similar seismic waves but on a smaller scale and intensity, so the loess will behave in the same way (Zhang et al., 2005).

Seismic settlement of loess is also affected by loess plasticity. Loess with a higher plastic index develops lower seismic residual strains, when subjected to dynamic loading. This was tested through loess samples of 8 to 16% plasticity index subjected to 100 kPastress applied in 10 cycles (Yuan and Wang, 2009).

The elastic modulus (E_0) of loess appears to play the largest role in how much seismic settlement loess can undergo. It was found that no large seismic settlement will happen when loess is subjected to strong seismic waves as long as the elastic modulus is above 100 MPa. As such, knowledge of elastic modulus can assist determining the level of deformation resistance in the plastic phase (Yuan and Wang, 2009).

In modern day Chinese engineering design codes it is conventional practise to include collapsibility assessments and prevention. The study carried out its investigation to find if there was a relationship between seismic settlement and collapsibility in loess by using data from the microstructure of loess.

As previously mentioned, there are large similarities between British loess and Chinese loess and one of the parameters in that discovery was the analysis of the loess' microstructure, meaning that the results of this investigation can be applied to the HS2 project, as well as possibly adopting some of the Chinese design codes when building on top of loess.

1.2SMALL STRAIN STIFFNESS

Small strain stiffness, or G_{max} , and strain dependant stiffness are parameters used to explain the small strain behaviours of soil and are inputsin to advanced soil models including the Hardening Soil Small Strain model (HSS).These parameters are either measured by using advanced triaxial testing(direct measurements) or semi-empirical equations(indirect derivation).

Using the HSS model has become more popular than widely used Mohr-Coulomb model (MC),as MC does not take strain dependant stiffness behaviour in to account and fall short in accurate estimation of ground movements upon change in stress state. The MC model also only utilises the Young's modulus and doesn't differentiate between loading and unloading stiffness. The HS model utilises triaxial unloading and reloading secant stiffness, triaxial loading stiffness, and oedometer loading tangent stiffness, to offer a better incite in to serviceability of ground systems.

The HSS models go further to use a wider suite of interdependent parameters including void ratio (e), the average size of quartz grains, the shape of the particles, carbonates which are attached with clay minerals, the effective stress (σ'), and distribution of grains and intergranularspaces,inconjunction with proxy parameter for sediments origin and final deposition history. Soils that share common characteristics as a result of having similarities in their formation, in theory could display relatively the same small strain stiffness behaviour. Assadi-Langroudi (2019) recently proposed a Provenance-Transport-Deposition (PTD) model for loess in England to show the portability of ground properties across loessic sites.

Use ofG_{max} in designis beneficial,particularly when designing structures that generate shear waves in to engineering ground, such as railways; it is necessary to know whether or not these waves cause ground movements in the soil. If soil has a low G_{max} the shear waves being imposed on the soil can potentiallycause ground movement to occur, which in the case of loess can lead to collapse, sudden settlement, or even uplift, affecting the serviceability of the superstructure.

1.3MEASUREMENT OF SMALL STRAIN STIFFNESS

1.3.1Semi-empirical methods

Hardin (1978) formulated G_{max} (small strain stiffness) in Equation 1,

$$\frac{G_{max}}{P_a} = S.F(e).(P'/P_a)^n \text{ Eq. 1}$$

Where $F(e)$is a function of soils void ratio; P' is the mean effective stress which represents the relationship between the small strain stiffness and its reliance on the stress state of soil. The inclusion of atmospheric pressure, P_a, to be used as a reference stress allows the parameter S to become dimensionless and is used to identify the nature of the soil.

Hardin and Richart (1963) used initial void ratio $e_0$in investigating the small strain stiffness of sands, for clay soils however, the normalvoid ratio must be used in establishing the value of $F(e)$. The void ratio function used and the atmospheric pressure will determine the value of the stress multiplier, S.

Hardin and Black (1968)suggested that a relationship between mean effective stress and G_{max} existsand expressed it in the form(Khosravi et al., 2010):

$$G_{max} = 625 \times OCR^k.F(e)\sqrt{P_a\sigma'_m} \text{ Eq. 2}$$

Wherekrepresents the soils plasticity, and $\sigma'_m$is the mean effective stress which uses the same units as the atmospheric pressure and G_{max}; OCR is the over-consolidation ratio. In this work, ground data from the study site in Faversham is processed with Equation 2 to build an alternative profile of small strain stiffness. Equation 3 is also commonly used in approximation of , although shear modulus differs from small strain stiffness in being valid at large strains only.

$$E_t = G * 2(1+\nu) \text{ Eq. 3}$$

Where ν is the Poisson's ratio, and Young's tangent modulus $E_t$is normally derived from stress-strain diagram from a compression triaxial test or unconfined compression(Cox and Mayne, 2019).

Khosravi and McCartney (2009) proposed Equation 4 for determination of G_{max} for compacted soils,

$$G_{max} = A \times F(e) \times (\sigma'_m)^n Eq. 4$$

It is worth mentioning that this method is not well suited to calculating G_{max} for loess as it is meant to be used for compacted soils, and since the data used is from alluvial deposits it does not really fit this criteria. However, since this is being used to build a vertical profile it is still possible to beusedfor loosely packed loess-like sediments(Khosravi et al., 2010). To obtain the values of A and n,theslope and interception of the best fit line for variation of $log\frac{G_{max}}{F(e)}$ with $log\,\sigma'_m$can beused.Both A and n are used as fitting parameters for Eq. 1.

1.3.2 Direct measurement

Measurement of engineering properties ofloess soil is best to be undertaken in fieldas retrieving undisturbed samples and measuring them in a laboratory is incredibly difficult. Measuring G_{max} for loess directly requires either bender element test,resonant column test, or seismic cone penetration test. Test used to find shear elastic modulus and damping characteristics of soils. A soil sample is placed in a cylinder where the bottom of the container is fixed and the top is able to disturb the sample through longitudinal or torsional vibrations, where the soils response is then measured. An electromagnetic drive system is used to generate these vibrations with varying frequencies. This test is used to find the same desired data as an RC test but uses a different method. A CPT probe is placed in to the soil at a desired depth to generate a seismic wave by hitting the seismic plate using a sledgehammer. The shear waves will pass through the soil and stimulate the accelerometer on the CPT probe which then displays the data. Bender element involves using different kinds of tests through loading. The types of loading involved are hoop tension loading, longitudinal tension loading, and maximum shear loading. These results are then translated to generate the maximum small strain stiffness of a soil.

II. MATERIALS AND METHODS

2.1STUDY AND STRATIFICATION

2.1 BENCHMARK SITE

The site adopted for this study is a previous Brickearth quarry (currently farmland) located in south west of Faversham, and confined between A2 trunk road from South and Faversham-Sittingbourne railway line from North, at National Grid Reference E599671 N161189. Geological and Geotechnical data collated and reported here are made available by the British Geological Survey and borehole log data presented in Zourmpakis et al. (2006). The area is at the boundary of patchily distributed Head Brickearth and superficial fine alluviums with brickearth soils reaching maximum depth of 3.7m forming an upper non-calcareous loessicbrickearth on a lower calcareous brickearth overlaying the Thanet Sand Formation. Table 1 and Figure 4 summarize mineralogical and physical properties of brickearth.

Table 1. Physical and mineralogical characteristics of loessic sequences in the benchmark site (data appeared in Assadi-Langroudi 2019; Milodowski et al. 2015; Zourmpakis et al. 2006; Northmore et al. 1996; Gruhn et al. 1974)

		Loessic sequences										Base	
		Upper Sequence							Lower Sequence			Thanet sand	
Depth: mbgl		0.6	0.8	1.1	1.3	1.5	1.8	2.0	2.2	2.4	2.9	3.4	3.7
Physical properties	Water content: %	20.5	18.2	18.7	17.9	20.1	19.1	14.9	14.4	10.9	11.9	17.5	19.9
	Specific Gravity	2.74	2.61	2.65	2.71	2.60	2.70	2.71	2.71	2.71	2.65	2.69	2.68
	Plasticity Index: %	16.0	14.0	11.0	13.0	17.0	13.0	9.0	6.0	NPI	NPI	12.0	11.0
	Void ratio	0.72	0.61	0.68	0.71	0.72	0.73	0.75	0.74	0.64	0.72	0.64	0.64
	Unit weight: kN.m-3	19.1	19.1	18.7	18.7	17.2	18.6	17.7	17.8	18.3	17.3	19.3	19.6
Grain size distribution	>2mm: %	0.00	0.10	0.00	0.00	0.10	0.00	0.00	0.00	0.10	11.3	0.00	0.70
	63μm-2mm: %	5.5	11.4	11.2	20.2	16.5	15.8	18.1	16.5	26.9	34.9	21.6	12.0
	63μm-2μm: %	69.9	58.7	61.5	60.6	48.9	54.0	43.0	68.6	55.5	35.4	21.6	12.0
	<2μm: %	24.6	29.8	27.3	19.2	34.5	30.2	38.9	14.9	17.5	18.4	21.6	18.4
	Pronounced size: μm	32-40										-	-
Mineralogy	Calcium Carbonate: %	-	-	-	-	-	-	-	12.8	8.7	4.0	0.5	0.5
	Kaolinite: %	6.3	5.1	4.5	3.2	4.9	4.9	5.1	4.7	4.5	5.2	5.1	5.1
	Smectite: %	0.7	0.7	1.1	1.7	1.5	1.6	1.3	1.0	1.5	1.2	2.6	2.6
	G_{max} : MN/m-2	310	220	180	240	120	110	80	190	90	120	180	220

It appears that plasticity across the two brickearth sequences generally decrease with depth as represented in Figure 4(b). This is can be attributed to the higher clay content in the upper brickearth sequence and also the calcium carbonate inclusion in the lower brickearth layer. It is clear that as the clay content in the soil decreases with depth so does the plasticity. Once the soil profile reaches enters the Thanet Sand formation, the clay content increases again resulting in an increased plasticity.

As one would expect, the water content in the upper brickearth and the Thanet Sand is higher than that of the lower brickearth, as shown in Figure 4(d), mainlydue to the higher plasticity of the soil in these two sections. As water content increases in soil, so does the soils plasticity. The high specific surface of clay platelets lead to elevated levels of net negative charge and hence plasticity and water retention capacity. Calcium Carbonate in soil led to a structure as porous as the clayey brickearth (Fig. 4a); the marked lower water retention capacity (Fig 4d) and plasticity may be attributed to the non-clastic and moderate solubility of carbonate bonds in loess.

Figure 4(c) shows the vertical profile for the bulk unit weight of the soil. The bulk unit weight decreases with depth;this is in good agreement with trends seen in Figure 4(d). Once the soil reaches the Thanet sand boundary bulk unit weight appears to increaseas the water content.

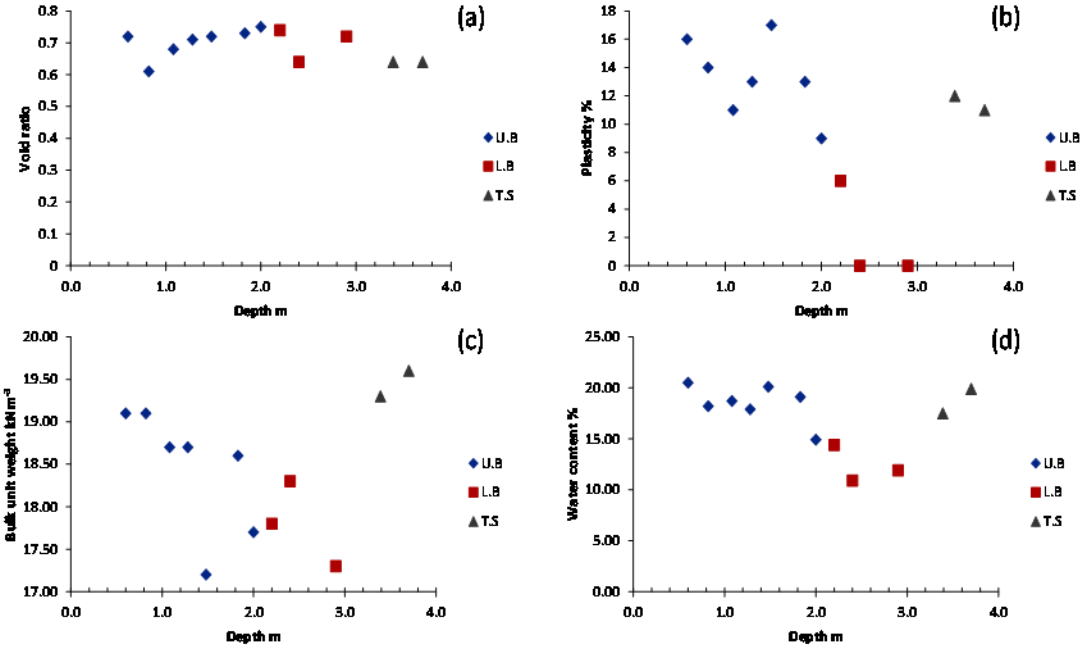

Fig. 4Variationwithdepth of physical soil parameters for upper non-calcareous brickearth, lower calcareous brickearth, and Thanet sand; (a) void ratio; (b) plasticity; (c) bulk unit weight; (d) water content

2.2 METHODS

As discussed in section 1.3,Equation 1 and Equation 2 are suited for cohesive soils to determinethe shear wave velocity,V_s. Also as previously discussed the $F(e)$function used in this equation is dependent on the type of soil. Likitlersuang et al., (2012) revisited and collated various $F(e)$functions for various soil types of range of packing states (i.e. porosity). The appropriate function is adopted from this seminal work and deployed to produce depth profiles of shear wave velocity and small-strain stiffness.

Table 2, Parameters used for calculating the small-strain stiffness depending on soil type; (Likitlersuang et al., 2012):

Soil type	Test method	S	$F(e)$	n	Void ratio range	References	Model
Remoulded kaolin	RC	327	$\frac{(2.973-e)^2}{1+e}$	0.5	0.76–0.9	Hardin and Black (1968, 1969)	
Reconstituted NC kaolin	RC	450	$\frac{(2.973-e)^2}{1+e}$		1.1–1.3	Marcuson and Wahls (1972)	
Reconstituted NC bentonite	RC	45	$\frac{(4.4-e)^2}{1+e}$	0.5	1.6–2.5	Marcuson and Wahls (1972)	
Several undisturbed silts and clays (NC range)	RC	74–288	$\frac{(2.973-e)^2}{1+e}$	0.46–0.61	0.4–1.1	Kim and Novak (1981)	SS1
Undisturbed NC clay	Cyclic TX	14	$\frac{(7.32-e)^2}{1+e}$	0.6	1.7–3.8	Kokusho et al. (1982)	
Six undisturbed Italian clays	RC & BE	275–1174	$e^{-1.3}$ $(averagefrome^{-x}: x = 1.11-1.43)$	0.40–0.58	0.6–1.8	Jamiolkowski et al. (1994)	
Several soft clays	SCPT	500	$e^{-1.5}$	0.5	0.5–5	Shibuya and Tanaka (1996)	SS2
Several soft clays	SPCT	1070–3080 (average 2400)	$(1+e)^{-2.4}$	0.5	0.5–5	Shibuya et al. (1997)	SS3

In Table 2, RC denotes resonant column test, Cyclic TX represents cyclic triaxial test, RC & BE signifies resonant column and bender element test, and SCPT means seismic cone penetration test.

Through using RC, Cyclic TX, RC & BE, and SCPT; these parameters were identified due to the constants of empirical relationship for small strain stiffness for clays, Equation 1; although in Jamiolkowski, Lancellotta, and Lo Presti(1994) calculations, σ'_vandσ'_hwere used in place of P′ and in Shibuya and Tanaka (1996), and Shibuya et al(1997) $\sigma'_v$was used rather than P′. P′represents the mean effective stress.

From Table 2 it is clear through the process of elimination that the best suited method for calculating the void ratio function is:

$$F(e) = \frac{(7.32 - e^2)}{1 + e} \text{Eq. 5}$$

As this method suits undisturbed silts and clays (NC range). This soil type is deemed closest to the loess in Faversham;both soils are undisturbed and both consist of silts and clays.

Other elements that can be found from Table 2 for several undisturbed clays and silts are S, n, and e. In the case of characterising the soil in terms of a number the given range is 74-288, an assumed number from this range will be used in the equations to calculateG_{max}. For the size of the particles another range is given, 0.46-0.61, the assumed range for this should be the number closest to the Faversham data, which in this case is 0.46. As for the void ratio range which is 0.4-1.1, the most appropriate number would be one that reflects the Faversham data best. In this case, as all the void ratios are within the range they can be used in the calculations.

Faversham loess is clayey and as such may come under the soil type category of several soft clays as well. This will lead to different values ofS, n, and $F(e)$. There are two methods for calculating these factors for several soft clays. The first will include S being 500 as this is a given variable, n being 0.5 as this is also given, and finally $F(e)$being:

$$F(e) = e^{-1.5} \text{Eq. 6}$$

The second method will include S being 2400 as this is the average for soils within this range, n 0.5 as this is again given, and $F(e)$will be:

$$F(e) = (1 + e)^{-2.4} \text{Eq. 7}$$

For all of these methods the void ratio range will be kept the same. The atmospheric pressure depends on the altitude;here it is assumed 100 kPa,,the common value for P_a.

III. RESULTS AND DISCUSSION

The shear wave velocity and small strain stiffness presented in this section are derived using the information in Table 2 to build a vertical profile for G_{max} using Eq. 1.For the SS1 (see Table 2) method,S, n and P_a are taken as 200, 0.46, and 100kPa. For the SS2 (see Table 2) and the SS3methods(see Table 2), S, n and P_a are taken as 500, 0.5, and 100kPa.

In Fig. 9, the deeper the soil the higher the small strain stiffness, in fact the top layer of the upper brickearth has half the small strain stiffness of the lower brickearth. This is because G_{max} is directly correlated with mean effective stress, (a function of bulk weight and depth).

These results infer that the upper brickearthmay generate substantial deformation upon transient loading which ties in with the high clay content in this layer. The fabric rearrangement and plastic behaviour that the upper brickearth exhibits most likely means that the top layer of soil does not possess high enough tensile strength in order to be suitable for engineering work.

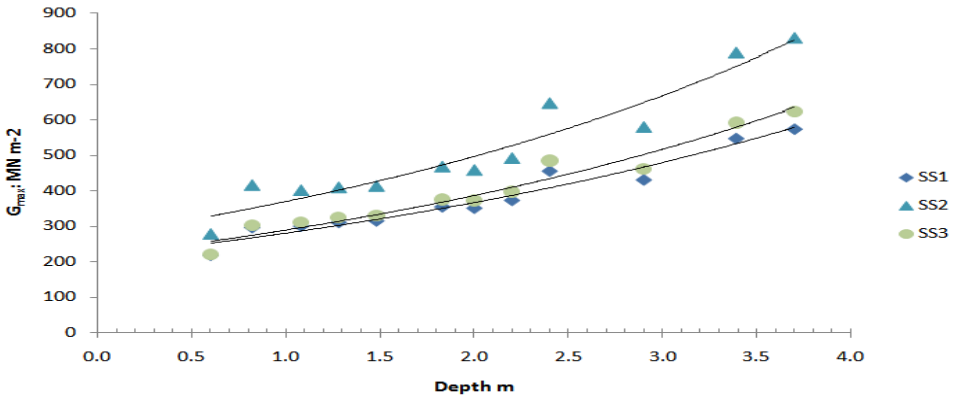

Fig. 9 G_{max}resultsplotted against depth using Hardin (1978) method

In Fig. 10 and Fig. 12one should take note that the drop in G_{max} reaches its lowest deficit at around 2 meters depth for most of the analytical methods. This is also where the soil has been identified to have

calcareous cementation, referred to as the lower brickearth. The small strain stiffness throughout this region seems to stay at this consistent level until around 2.9 meters. This is also where the lower brickearth region ends and therefore where the calcareous cementation ends. Beneath this depth and through the Thanet Sand, G_{max} increases Thanet Sand is cemented by kaolinite and smectite, both are clay minerals. These minerals connect angular sand particles, retain the friction,and leads to higher G_{max} orders.

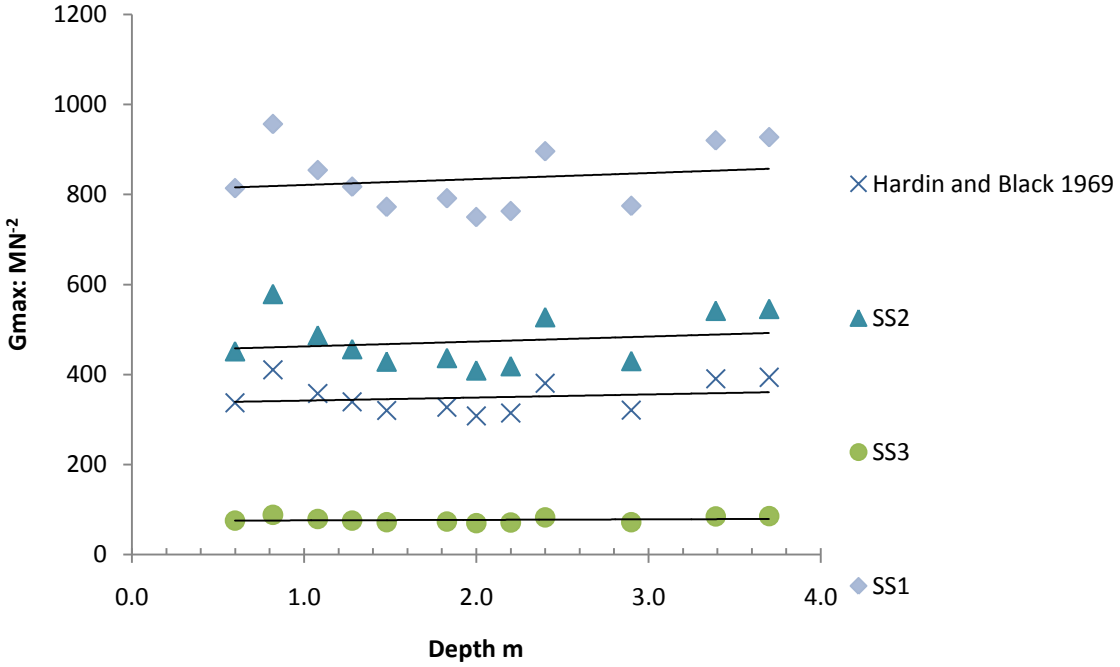

Fig. 10 G_{max}results plotted against depth using Hardin and Black (1968) method

In Figure 11, normalised$\mathbf{G_{max}}$is plotted against mean effective stressand offers theAvalue for Equation 4.

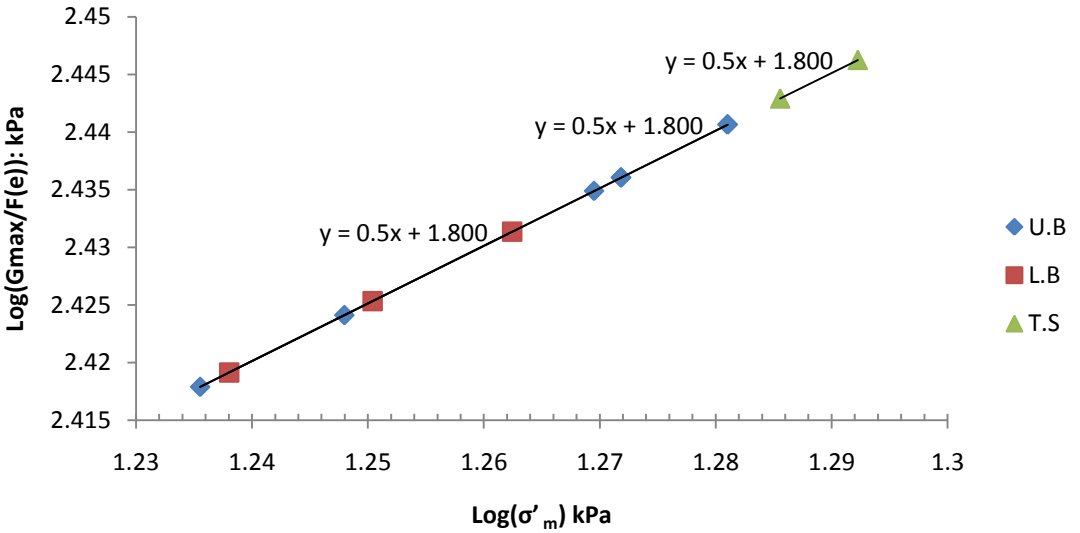

Fig. 11 G_{max}against normalised of mean effective stress

Figure 12 presents the variation of $\mathbf{G_{max}}$with depth using Khosravi and McCartney 2009 for loose soils; this method is arguably not suitable for this soil profile.

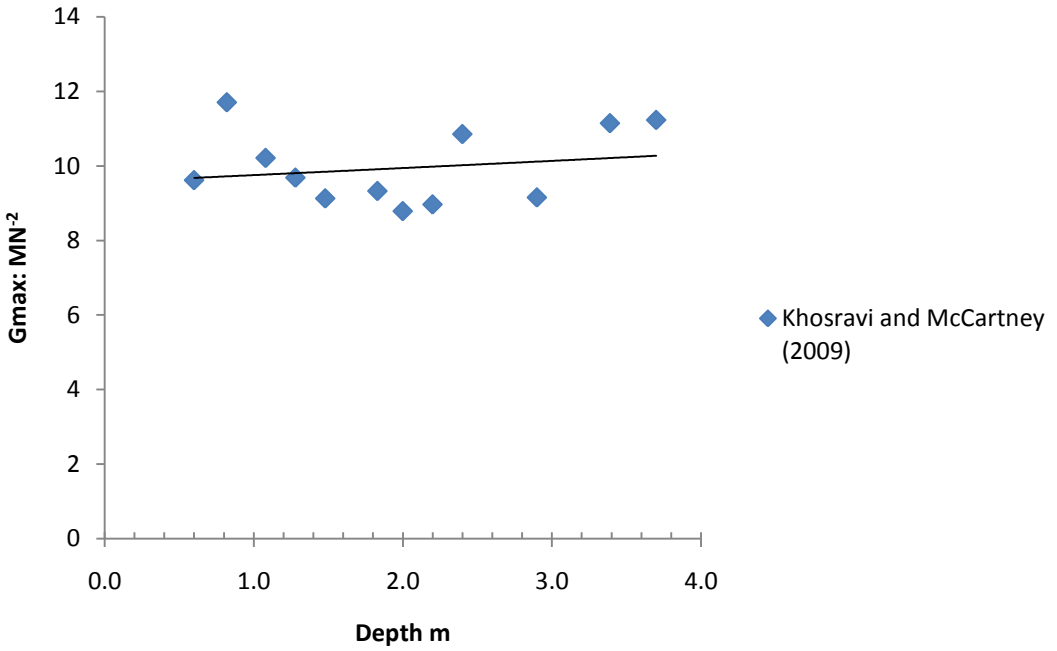

Fig. 12 G_{max}results plotted against depth using Khosravi and McCartney (2009) method

Generally small strain stiffness increases with depth and the effective stress; this is however not as explicit as one would hope in Fig. 12. There is a clear indication that the presence of the calcareous cementation is having an impact on the loessG_{max} in a negative way. This is probably because the calcareous cementation is made up of calcite with a rhombus shape and particles stacked on top of each other forming sheets. This does not provide the friction that a clay cementation would, making calcareous soils susceptible. The brittle nature of calcareous material offered by the honeycomb clay structure and the edge-to-face connections of clay platelets high enough stress or imposed movements.

Looking at Table 1 it can be seen that the clay content decreases with depth through the top 1.3m profile before adopting an increasing trend to the bottom of the upper sequence. Clay content is generally lower within the lower sequence and increase with depth. This trend can be followed in Fig. 12, suggesting a direct correlation between small strain stiffness and clay content.

Clay is the cementing agent within the upper brickearthand the porosity is generally low; this infers that upon flow through this layer, the cementation maycollapse;adding to collapse of the trellis pores due to increased density as a result of saturation, or the water will be forced in to voids in the soil. As discussed earlier, micro-pores provide suction in loess hydrodynamic forces may also influence the stability of trellis pores, which is where loess receives most of its tensile strength. If these voids were to be filled with water they will no longer be able to provide suction with implications on soils tensile strength. Collapse at depths as such can result in lower small strain stiffness. These factors need to be taken in to consideration with the fact that loess soil possesses trellis pores and how reliant the soil is on suction in order to generate tensile strength. This is because introducing this loading and unloading action will result in displacement of the clay particles and potentially the silt particles, which could cause these trellis pores to collapse.

Following densification, soil becomeslessporous,and pore water pressure experiences an excess pore water pressure, impacting the effective stress and stability of top soil overall.

While it is unlikely that the calcium carbonate in the lower brickearthis affected by water inflow,wetting could potentially affect the cementationand can cause further collapses.

3.1 THE EFFECTIVENESS OF SMALL STRAIN STIFFNESS

Equation8 is used to take the G_{max} values derived by the semi-empirical equations and translates itin to shear wave velocity. Generally, imposed shear waves (upon loading) that exceedsshear wave of loessic sequences may cause disturbance in the ground.

$$\frac{\sqrt{G_{max}}}{\sqrt{\rho}} = V_s \quad \text{Eq. 8}$$

Figure 13, 14, and 15captures the data from Figure 9, 10, and 12and demonstrate the depth profile of shear wave velocity.

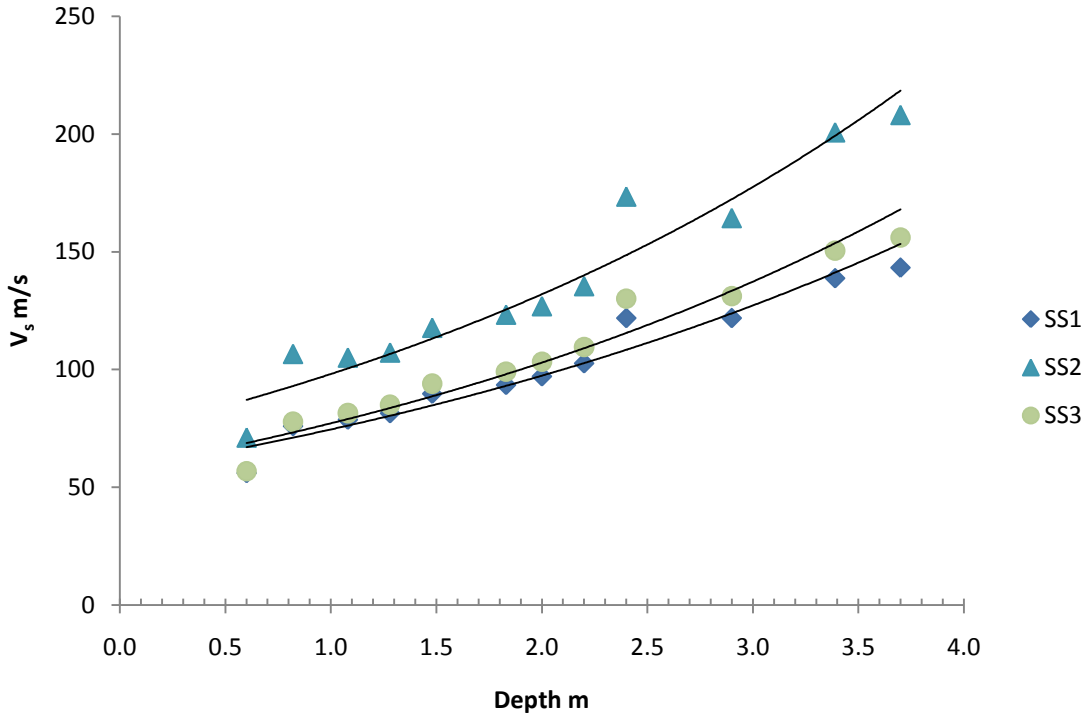

Fig. 13 $V_s$against depth using Hardin (1978) method

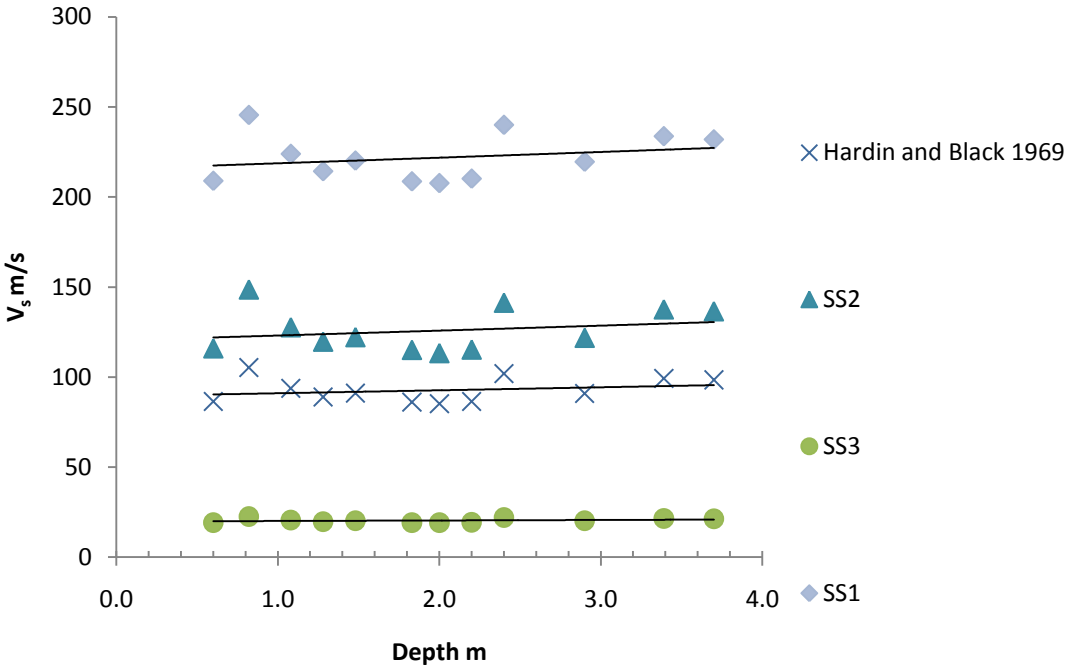

Fig. 14 $V_s$against depth using Hardin and Black (1968) method

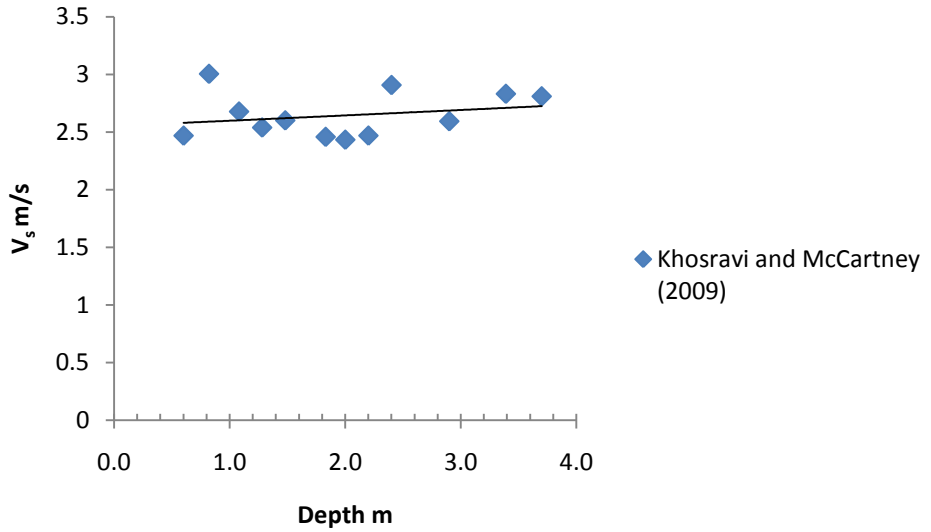

Fig. 15 $V_s$against depth using Khosravi and McCartney (2009) method

In Figure 16 G_{max} is directly measured using the shear wave velocity recorded in-situ and processed with Equation 8, thereby referred here as measured small strain stiffness.

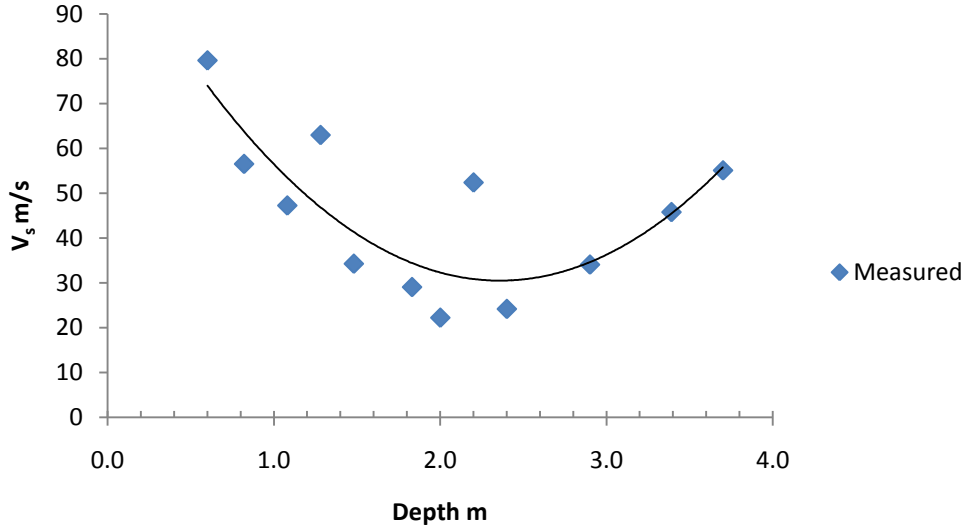

Fig. 16 Measured$V_s$against depth

A large discrepancy between estimated G_{max} through semi-empirical correlation (Fig. 13-15) and measured G_{max} (Fig. 16) is evident.

Thediscrepancycould be due to the choice of variables inEquation 1 used to calculate G_{max} . It appears as though the effective stress is being overcompensated for in the Equation 1. The depth has direct impact on P′and therefore G_{max} ;this is potentially where the inaccuracy is stemming from. This is particularly noticeable in Figure 13; Figures 14, 15, and 16 shows a decline in shear wave velocity once the soil sample entered the calcareous layer, illustrating more realistic account of small strain stiffness. Normalisation of G_{max} in Equation 1 against depth may offer a more accurate picture.

Findings are generally consistent with the recent work of Archer and Heymann(2015), in which small strain stiffness was deployed to predict the settlement of shallow foundations on sand.
They showed a discrepancy when comparing the measured and calculated G_{max} values (Fig 17-18).

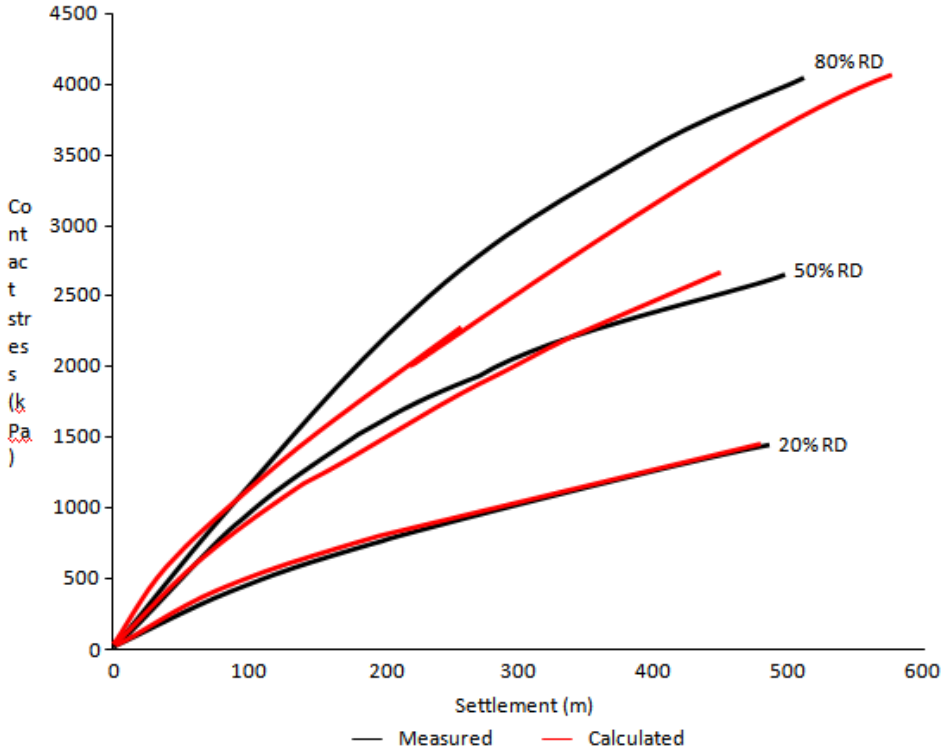

Fig. 17 Discrepancy of measured settlement and predicted settlement for sand (Archer and Heymann, 2015)

These confirm existence of some inconsistencies when calculating G_{max} .

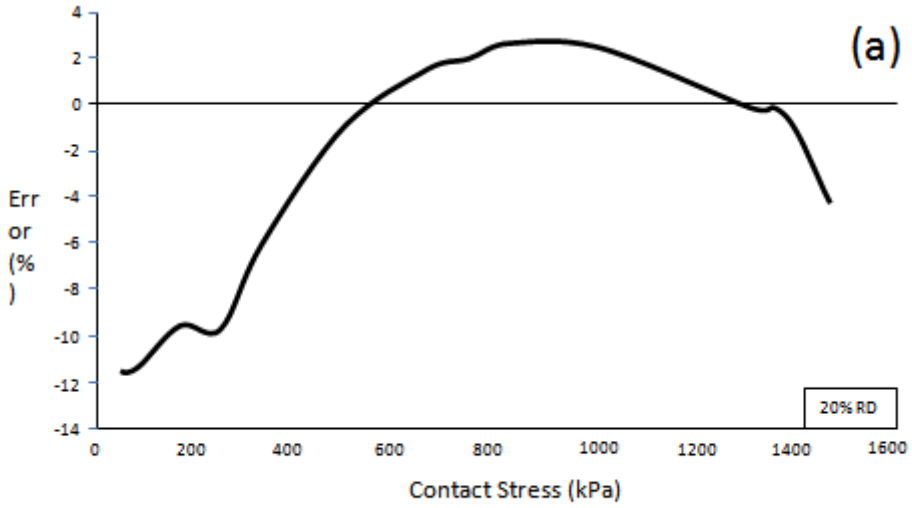

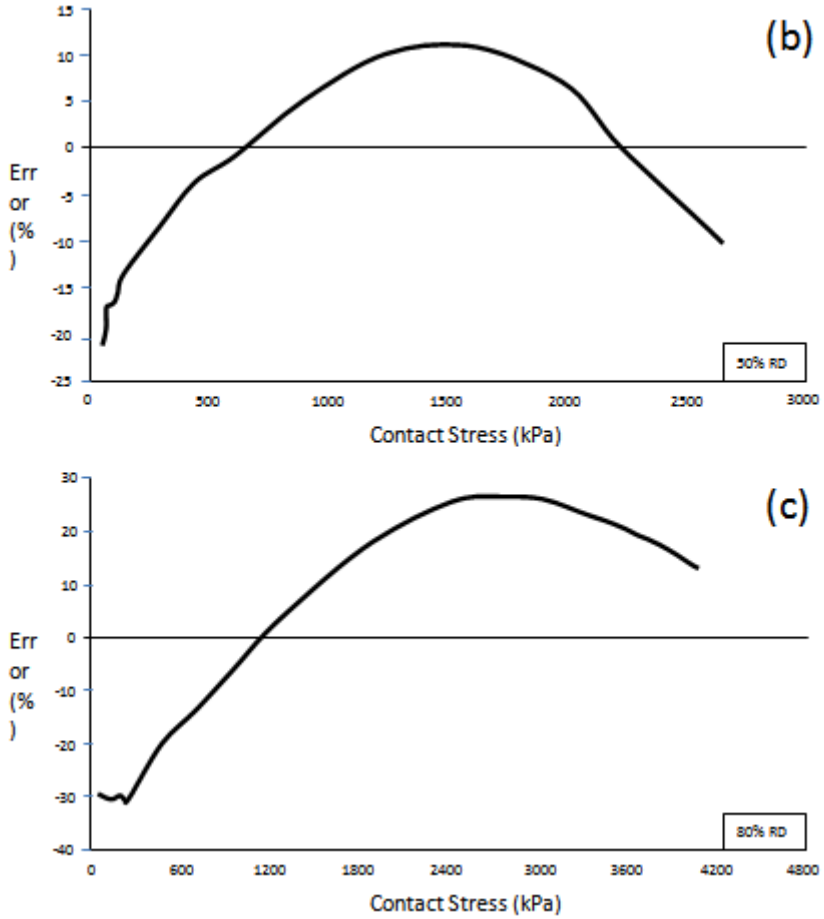

Fig. 18(a-c) Margin of error when predicting sand settlement (Archer and Heymann, 2015), (a) 20% relative density, (b) 50% relative density, (c) 80% relative density

Figure 17 and 18 it is clear that the inconsistency between measured and estimated values increase with the density of the soil.

Loukidis and Salgado used finite element simulations to test the effect of relative density and stress level on bearing capacity of footings on sand. These simulations show that for dense sand full formation of the general shear mechanism results in a considerably large amount of settlement; with a limit load range of 5-30% which is dependent on sand intrinsic properties and the relative density. This explores a connection between the relative density having an influence on G_{max} ; potentially explaining the margin of error in Fig. 18(a-c).

Higher sand content generally leads to a higher G_{max} ,owing to interlocking effect in granular mediums. It is possible that the reason for this inaccuracy of measured and predicted G_{max} in both papers is a result of the Equation 1, Equation 2, and Equation 4 not accounting for the soils characteristics when the contents of the constituents change affecting the mechanics of the soil. Particle characteristics affecting G_{max} is reinforced by Seed and Idriss (1970) who suggested that relative density does affect G_{max} , Iwasaki and Tatsuoka (1977) who proposed coefficient of uniformity can affect G_{max} , and Lo Presti et al., (1997) who put forward that mineralogy and grain angularity can also affect G_{max} . It can then be assumed that this is the cause for the discrepancy between the measured and calculated G_{max} .

IV. SMALL STRAIN STIFFNESS DEGRADATION

Soil becomesgraduallyweaker with each cycle of traffic loading/unloading and weather cycles. This is generally known as small strain stiffness degradation.

The freezing and thawing of pore water which has penetrated in to the soil will cause reduction in small strain stiffness. Water gets trapped within the pores and forms ice crystals, which then attract more water along the thermal gradient causing ice lenses to grow. Water traversing the soil to these ice lenses causes soil contraction as the removal of water from other areas reduces the soils volume. As a result of this, the locations of the ice lenses in the soil expand due to the increase in water content. This leads cracks to form which will increase in depth and girth with each freezing and thawing cycle. The extent and likelihood of degradation hence increase with water retention capacity, plasticity and clay content. This appears in Fig. 19.

For both sequences, the reference threshold shear strain ($\gamma_{0.7}$) is determined from the stiffness degradation curve, which is plotted using the rigorous method of [27], taking into account the mean field effective confining stress, void ratio and plasticity index (Fig 19a). Measured $\gamma_{0.7}$ is expressed in form of an exponential function of plasticity index (PI) in Fig 19(b), which then can be used alongside G_{max} in capacity of input parameters needed in Hardening Soil Small Strain HSS models.

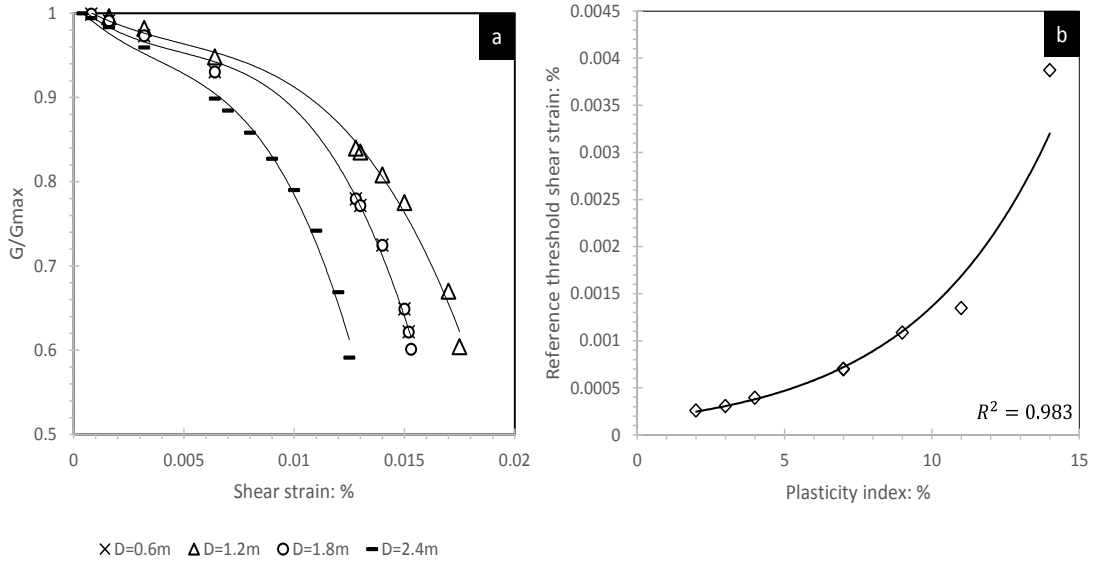

Fig. 19(a) Modulus reduction curve (stiffness degradation) at [very] small strain range for upper sequence (D=0.6, 1.2, 1.8mbgl) and lower sequence (D=2.4m). (b) Exponential best-fit of $\gamma_{0.7}$ versus plasticity index for both upper and lower sequences

Modulus reduction curve is reproduced in Fig. 20 for upper non-calcareous sequence (D=1.08mbgl - a) and lower calcareous sequence (D=2.20mbgl - b). The graphs illustrate the strain- softening of soils on the stress-strain response plot, following the approximation of non-linear and hysteretic stress-strain behaviour under cyclic traffic loading, using the modified Kelvin-Voigt model [28]. The brittle response of cemented loess to strain is apparent on comparing the two diagrams.

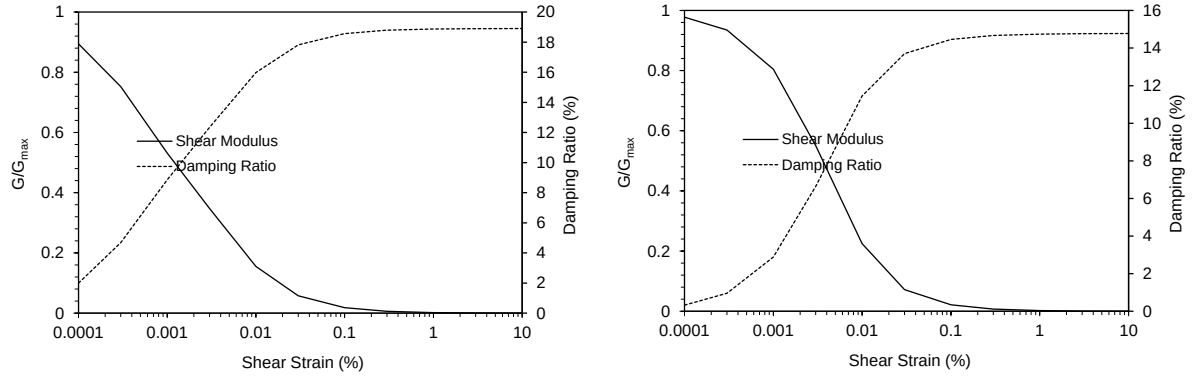

Fig. 20 Iteration of shear modulus and damping ratio with shear strain for 10 cycles of loading (a) upper decalcified sequence (b) lower calcareous sequence

Fig. 20 Iteration of shear modulus and damping ratio with shear strain for 10 cycles of loading (left) upper decalcified sequence (right) lower calcareous sequence.

A popular way of calculating G_{max} at very small strains is using Ishibashi and Zhang (1993) matrix, but there are alternatives such as Viggiani (1992) and Rampello et al. (1997).

V. CONCLUSION

Small strain stiffness in cemented loess appears relatively lower than that of non-calcareous loess. The lower stiffness of calcareous loess, in part, is due to the presence of carbonate sands of limited crystalline integrity and sub-rounded texture. Small strain stiffness increases with depth in cemented loess. This pattern justifies, to some extent, the suitability of cemented loess as a subgrade to future embankments for their lower punching shear risk. In evaluating the small strain stiffness through semi-empirical equations, the overburden

pressure plays key role, leading to a direct correlation between G_{max} and depth. This contradicts the trends seen for measured G_{max} values gained via direct measurement of shear wave velocity for calcareous cemented loess. The discrepancy is discussed here and is deemed to be controlled by particle characteristics.

ACKNOWLEDGEMENTS

Financial support for the work presented in this paper was provided by the National Research Foundation through the DST-NRF Fellowships for Early Career Researchers from the United Kingdom (NFPF170627245562).

REFERENCE

[1]. Archer, A. and Heymann, G. (2015). Using small-strain stiffness to predict the load-settlement behaviour of shallow foundations on sand. [online] Www.scielo.org.za. Available at: http://www.scielo.org.za/scielo.php?script=sci_arttext&pid=S1021-20192015000200004 [Access 21 Jan. 2019].

[2]. Assadi-Langroudi, A. (2019). A conceptual model for loess in England: Principles and applications. [online] Science Direct. Available at: https://www.sciencedirect.com/science/article/abs/pii/S0016787818301731 [Accessed 11 Jan. 2019].

[3]. Assadi-Langroudi, A., Ng'ambi, S. and Smalley, I. (2018). Loess as a collapsible soil: Some basic particle packing aspects. [online] Science Direct. Available at: https://www.sciencedirect.com/science/article/pii/S1040618216301641 [Accessed 11 Jan. 2019].

[4]. Assadi-Langroudi, A. and Jefferson, I. (2013). COLLAPSIBILITY IN CALCAREOUS CLAYEY LOESS: A FACTOR OF STRESS-HYDRAULIC HISTORY. [online] Geomatejournal.com. Available at: http://www.geomatejournal.com/sites/default/files/articles/620-627-62312-arya-sept-2013.pdf [Accessed 8 Jul. 2019].

[5]. Barden, L., McGown, A. and Collins, K. (2018). The collapse mechanism in partly saturated soil. [online] Science Direct. Available at: https://www.sciencedirect.com/science/article/pii/0013795273900069 (Accessed 8 Dec. 2017).

[6]. Bardet, J.P., Ichii, K., and Lin, C.H. (2000) "Equivalent-linear Earthquake site Response Analyses of Layered Soil Deposits EERA." University of Southern California, Department of Civil Engineering

[7]. Cox, C. and Mayne, P. (2019). Soil stiffness constitutive model parameters for geotechnical problems: A dilatometer testing approach. [online] Geronline.com. Available at: https://www.geronline.com/file/document/12%20-%20Cox%20Mayne%20-%20Final%20Revised%2021%20May.pdf [Accessed 13 Mar. 2018].

[8]. Gruhn, R., Bryan, A. and Moss, A. (1974). A Contribution to Pleistocene Chronology in Southeast Essex, England. [online] Science direct. Available at: https://www.sciencedirect.com/science/article/pii/0033589474900635 [Accessed 13 Mar. 2018].

[9]. Hardin, B. O. (1978). "The nature of stress-strain behaviour for soils." Proc.. Earthquake Engineering and Soil Dynamic, ASCE, New York, June, 3-90.

[10]. Ishibashi, I. and Zhang, X. (1993). 1993 Ishibashi& Zhang - G Gmax and Damping. [online] Scribd. Available at: https://www.scribd.com/document/63408565/1993-Ishibashi-Zhang-G-Gmax-and-Damping [Accessed 3 Jul. 2019].

[11]. Iwasaki, T. and Tatsuoka, F. (1977). EFFECTS OF GRAIN SIZE AND GRADING ON DYNAMIC SHEAR MODULI OF SANDS. [online] J-STAGE. Available at: https://www.jstage.jst.go.jp/article/sandf1972/17/3/17_3_19/_article/-char/ja/ [Accessed 8 Jul. 2019].

[12]. Jamiolkowski, M., Lancellotta, R. and Lo Presti, D. (1994). Remarks on the stiffness at small strains of six Italian clays. [online] Research Gate. Available at: https://www.researchgate.net/profile/Diego_Lo_Presti/publication/306157192_Remarks_on_the_stiffness_at_small_strains_of_six_Italian_clays/links/57e032ab08aece48e9e1f088.pdf [Accessed 5 Mar. 2018].

[13]. Khosravi, A., Ghayoomi, M., McCartney, J. and Ko, H. (2010). Impact of Effective Stress on the Dynamic Shear Modulus of Unsaturated Sand. [online] Unh.edu. Available at: http://unh.edu/geotech/papers/Khosravi%20et%20al.%202010%20GeoFlorida.pdf [Accessed 11 Jan. 2019].

[14]. Likitlersuang, S., Teachavorasinskun, S., Surarak, C., Oh, E. and Balasubramaniam, A. (2018). Small strain stiffness and stiffness degradation curve of Bangkok Clays. [online] Science direct. Available at: https://www.sciencedirect.com/science/article/pii/S003808061300067X [Accessed 13 Mar. 2018].

[15]. Likitlersuang, S., Teachavorasinskun, S., Surarak, C., Oh, E. and Balasubramaniam, A. (2012). Small strain stiffness and stiffness degradation curve of Bangkok Clays. [online] Science Direct. Available at: https://www.sciencedirect.com/science/article/pii/S003808061300067X#f0010 [Accessed 9 Jan. 2019].

[16]. Lin, C.Y. (1960), Structure of loess, Symposium on basic properties of loess, Civil Engineering and Architecture Institute of Chinese Academy of Sciences, Science Press, Beijing (Accessed 8 Dec 2017).

[17]. Lo Presti D.C.F., Pallara O. &Cavallaro A., 1997. Damping Ratio of Soils from Laboratory and In-Situ Tests Proc. XIV ICSMFE, Seismic Behaviour of Ground and Geotechnical Structures, Balkema, Rotterdam: 391-400

[18]. Loukidis, D. and Salgado, R. (2010). Effect of Relative Density and Stress Level on the Bearing Capacity of Footings on Sand. [online] Pdfs.semanticscholar.org. Available at: https://pdfs.semanticscholar.org/9421/91d57a97afa7a4ffc52643305f3ba9a84f17.pdf [Accessed 8 Jul. 2019].

[19]. Milodowski, A., Northmore, K., Kemp, S., Entwisle, D., Gunn, D., Jackson, P., Boardman, D., Zoumpakis, A., Christopher D.F., Rogers., Dixon, N., Jefferson, I., Smalley, I. and Clarke, M. (2015). The mineralogy and fabric of 'Brickearths' in Kent, UK and their relationship to engineering behaviour. Bulletin of Engineering Geology and the Environment. [online] Eprints.nottingham.ac.uk. Available at: http://eprints.nottingham.ac.uk/32571/1/brickearth.pdf [Accessed 12 Mar. 2018].

[20]. Northmore, K., Bell, F. and Culshaw, M. (1996). The engineering properties and behaviour of the brickearth of South Essex. [online] Research gate. Available at: https://www.researchgate.net/publication/245379013_The_engineering_properties_and_behaviour_of_the_brickearth_of_South_Essex [Accessed 13 Mar. 2018].

[21]. Rampello, S., Viggiani, G. M. B., and Amorosi, A. (1997). "Small-strain stiffness of reconstituted clay compressed along constant triaxial effective stress ratio paths." Géotechnique, 47(3), 475–489.

[22]. Seed, H. and Idriss, I. (1970). SIMPLIFIED PRO EDURE FOR EV LU TINGSOILLIQUEF TION POTENTI L. [online] https://www.scribd.com/document/385685982/Seed-e-Idriss-1970. Available at: https://www.scribd.com/document/385685982/Seed-e-Idriss-1970 [Accessed 6 Jul. 2019].
[23]. Shibuya and Tanaka (1996). Estimate of Elastic Shear Modulus In Holocene Soil Deposits. [online] jstage. Available at: https://www.jstage.jst.go.jp/article/sandf1995/36/4/36_4_45/_article/-char/ja/ [Accessed 5 Jul. 2018].
[24]. Vardanega, P. and Bolton, M. (2013). Stiffness of Clays and Silts: Normalizing Shear Modulus and Shear Strain. [online] civ.eng.cam Available at: http://www-civ.eng.cam.ac.uk/geotech_new/people/bolton/mdb_pub/226.pdf [Accessed 1 Apr. 2018].
[25]. Viggiani, G. (1992). City Research Online - Small strain stiffness of fine grained soils. [online] Openaccess.city.ac.uk. Available at: http://openaccess.city.ac.uk/7896/ [Accessed 5 Jul. 2019].
[26]. Wang, Z., Luo, Y., Guo, H., Tian, H. (2012) Effects of initial deviatoric stress ratios on dynamic shear modulus and damping ratio of undisturbed loess in China, Science Direct. Available at: https://www.sciencedirect.com/science/article/pii/S0013795212002050 (Accessed: 17 December 2017).
[27]. Wang, L., Zhong-xia, Y., Wang, J., Sun, C. (2000) Laboratory study of effect of dry density on seismic settlement of compacted loess--《EARTHQUAKE ENGINEERING AND ENGINEERING VIBRATION》2000年01期, En.cnki.com.cn. Available at: http://en.cnki.com.cn/Article_en/CJFDTOTAL-DGGC200001011.htm (Accessed: 15 December 2017).
[28]. Zhang, J., Andrus, R. and Juang, C. (2005) Normalized Shear Modulus and Material Damping Ratio Relationships | Journal of Geotechnical and Geoenvironmental Engineering | Vol 131, No 4, Ascelibrary.org. Available at: https://ascelibrary.org/doi/10.1061/%28ASCE%291090-0241%282005%29131%3A4%28453%29 (Accessed: 17 December 2017).
[29]. Zourmpakis, A., Boardman, D.I., Rogers, C.D.F, Jefferson, I., Gunn, D.A., Jackson, P.D., Northmore, K.J., Entwisle, D.C., Nelder, L.M., and Dixon, N. 2006. Case study of a loess collapse field trial in Kent, SE England. Quarterly Journal of Engineering Geology and Hydrogeology. 39, 131-150.

HaarisNobee-Fox" Small strain stiffness of loessic soils across South East England" International Journal of Research in Engineering and Science (IJRES), vol. 07, no. 3, 2019, pp.